Paper

The substrate-film lattice mismatch in $La_{0.7}Ba_{0.3}MnO_3$ thin films for uncooled infrared bolometric applications

Non-member Ken-ichi Hayashi (Keio University)
Non-member Eiji Ohta (Keio University)
Member Hideo Wada (Japan Defense Agency)

$La_{0.7}Ba_{0.3}MnO_3$ (LBMO) thin films known to colossal magnetoresistance were deposited for uncooled infrared bolometers. The optimum oxygen pressure was examined in the process of the laser ablated LBMO films, and films were deposited on $SrTiO_3$ (100), $LaAlO_3$ (100) and MgO (100) substrates under the optimum oxygen pressure. The lattice mismatch between these substrates and LBMO films changed the surface structure of films. In X-ray diffraction and atomic force microscope, the LBMO film deposited on $SrTiO_3$ (the LBMO/STO film) showed a high orientation for the substrate, and the grain growth of the LBMO/STO film was progressed. The temperature dependence of resistivity has a good agreement with that of LBMO bulk. In the near-room temperature, the LBMO/STO film showed a high TCR value, about 4 %/K. Moreover, TCR values of the LBMO/STO film were over 2 %/K from 300K to 335K. On the other hand, LBMO films deposited on $LaAlO_3$ and MgO substrates, having large substrate-film lattice mismatches, showed a low TCR value, below 2 %/K, in the near-room temperature.

Keywords: $La_{0.7}Ba_{0.3}MnO_3$, uncooled infrared bolometer, laser ablation, X-ray diffraction, atomic force microscope, temperature coefficient of resistance

1. Introduction

The $La_{1-x}A_xMnO_3$ (A: divalent alkaline-earth ions) system exhibiting colossal magnetoresistance (CMR) has recently generated much interest.[1] It has been exposed to the attention from not only academic research for the mechanism of CMR but also magnetic industries. Some of the applications of the CMR effect include those in read heads for magnetic information storage and low-field magnetic sensors. The transport properties of this system exhibit a transition from a paramagnetic insulating state to a ferromagnetic metallic state (I-M transition) with decreasing temperature. The correlation of magnetism and conductivity in mixed valence manganese perovskites was traditionally explained with the double exchange (DE) model.[2]~[5] In the model, the ferromagnetic interaction between Mn^{3+} and Mn^{4+} is established by the motion of charge carriers in the film with the help of oxygen anions. The observed properties are correlated with the Mn^{3+} : Mn^{4+} ratio. The ratio can be varied either by changing the concentration x of the component A or changing the oxygen stoichiometry.[6]

On the other hand, it has been reported that this system has sharp resistive change at the insulator-metal transition temperature (Tc) near room temperature.[7] This resistive change makes this system a candidate for uncooled infrared bolometers.[8] Materials represented as vanadium oxide (VO_x) having a high temperature coefficient of resistance (TCR: defined as 1/R dR/dT) near room temperature have been studied.[9] For uncooled infrared bolometer materials, TCR should be higher than 2 %/K, the TCR value of a conventional VO_x bolometer, in the temperature range of near room temperature.[10]

In this work, we present TCR properties of $La_{0.7}Ba_{0.3}MnO_{3-\delta}$ (LBMO) thin films, in particular substrate-dependent electric properties. At first, the optimization of oxygen condition in the films was carried out by measurements of microstructures and the electric properties. Substrate-dependent properties of LBMO thin films were investigated under the optimum oxygen pressure, and LBMO films were evaluated as uncooled infrared bolometers.

2. Experiment

2.1 **Sample Preparation** Thin films were deposited by a laser ablation (LA) of a ceramic target with a composition of $La_{0.7}Ba_{0.3}MnO_3$. An ArF excimer laser with a wavelength of 193 nm was used. The films were deposited on the $SrTiO_3$ (100), $LaAlO_3$ (100) and MgO (100) substrates at 500 ℃ under an oxygen pressure of 53.3 Pa. LBMO film deposition rates were approximately 20 nm/minute with total film thickness of ~ 200 nm. Annealing was performed at 900 ℃ under 1 atmosphere of oxygen for 30 minutes. The composition of the films were analyzed to be $La_{0.7}Ba_{0.3}MnO_{3-\delta}$ by electron probe microanalysis (SHIMADZU: EPMA-8705), and the composition slippage from the target was not confirmed.

2.2 **Measurements** The crystallinities of the films were characterized by X-ray diffraction (XRD) using the $\theta/2\theta$ scan (RIGAKU: RAD-RC). Cu Kα radiation was used from 20° to 80° with a step size of 0.01° and counting rate of 0.3 second/step. The current and voltage for the measurements were 200 mA and 40 kV, respectively. In this measurement, the angle θ of the goniometer was tilted -5° in order to reduce the influence of the single crystal substrate. For more advanced crystallinity evaluation, X-ray double-crystal rocking curves were measured. (SHIMADZU: PXD-400) The rocking curves were obtained with Cu Kα radiation. A germanium single

crystal was served as a monochromator. The step size was 0.001° , and the counting rate, 2 second/step. The current and voltage for the measurements were 35 mA and 40 kV, respectively. For the surface analysis we employed mainly atomic force microscope (SHIMADZU: SPM-9500) to observe the surface morphologies which influenced the electrical properties of thin films. Atomic force microscope (AFM) measurements were conducted in the contact mode at room temperature. The measurement range was 1×1 μ m^2. Each film was characterized by a four-point dc resistance measurement, and the results were used to calculate TCR.

3. Result and Discussion

3.1 Optimization of an oxygen pressure at deposition

Before discussions on the substrate-film lattice mismatch, the optimum oxygen pressure was examined.[11] In this examination, LBMO films deposited on the $SrTiO_3$ (STO) substrate (LBMO/STO films) under an oxygen pressure of 13.3-80.0Pa were selected. Fig.1 shows the oxygen pressure dependence of lattice parameters of LBMO/STO films. The film deposited under an oxygen pressure of 53.3Pa has the nearest lattice parameter of the STO substrate, which has the smallest substrate-film lattice mismatch. Surface morphologies of LBMO/STO films are shown in Figs. 2(a)-(f). The average grain size of the film deposited under an oxygen pressure of 53.3Pa is the largest [Fig. 2(d)]. It is considered to be the optimum oxygen pressure for the grain growth. Its resistivity also shows the minimum in Fig. 3. The case of oxygen pressures lower than 53.3Pa seem to make the oxygen deficiency state in a LBMO film, because films deposited in such oxygen pressures behave themselves like semiconductor or has a resistive peak at lower temperature. 53.3Pa is the oxygen pressure which cancels the oxygen deficiency in a LBMO/STO film. In this study, we aimed at the substrate-film lattice mismatch of the LBMO film without oxygen deficiency condition, so 53.3Pa was chosen as the optimum oxygen pressure at deposition.

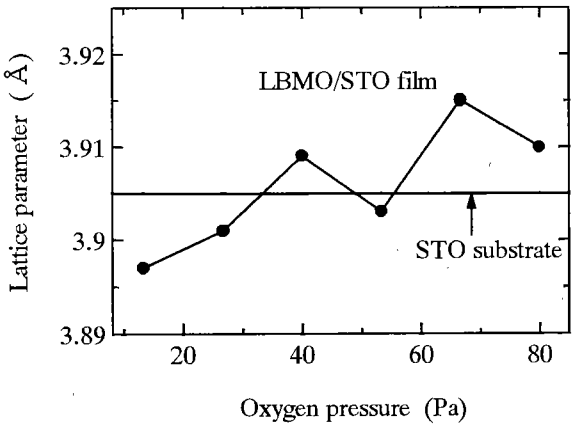

Fig. 1. Oxygen pressure dependence of lattice parameter for LBMO/STO films. Lattice parameters were calculated as pseudocubic.

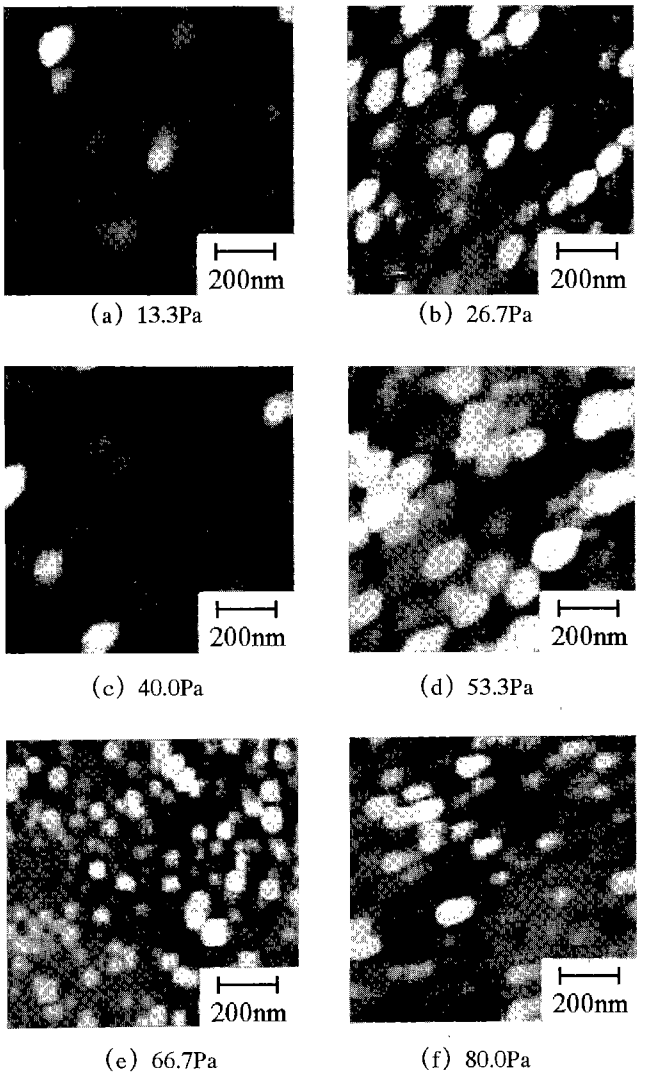

Fig. 2. (1 μ m)^2 AFM images of LBMO/STO films. (a)-(f) are images of films deposited under an oxygen pressure of 13.3-80.0Pa.

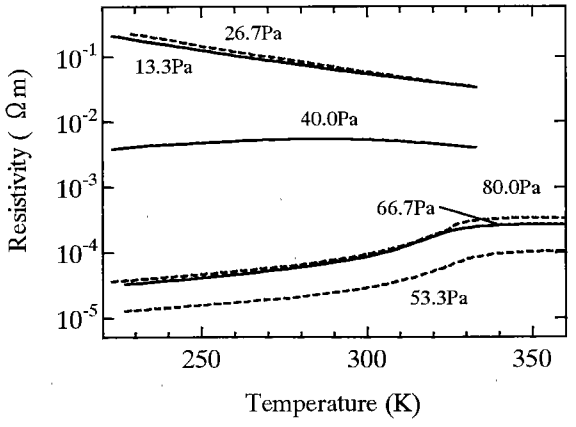

Fig. 3. Temperature dependence of resistivity for the LBMO/STO film deposited under an oxygen pressure of 13.3-80.0 Pa.

3.2 **Crystallinity** X-ray diffractograms using $\theta/2\theta$ scans of the LBMO bulk (used as the LA target) are shown in Fig. 4 (a), and LBMO films deposited on the $SrTiO_3$ (STO), $LaAlO_3$ (LAO) and MgO are shown in Figs. 4(b), 4(c) and 4(d), respectively. The LBMO bulk pattern corresponds to no preferential orientation. Lattice parameters are indicated in Table 1. Lattice constants were calculated as pseudocubic. The substrate-film lattice mismatch is smaller than the value expected from the lattice mismatch between substrate and bulk (the substrate-bulk lattice mismatch). In the growing process of LBMO films, the substrate-film lattice mismatch seems to be smaller than the substrate-bulk lattice mismatch. The substrate-film lattice mismatch greatly decreases, as the substrate-bulk mismatch is bigger. The substrate-bulk lattice mismatch of the LBMO film deposited on MgO (the LBMO/MgO film) is so large that dislocations are formed, and these dislocations seem to relax the substrate-bulk lattice mismatch in a region near the interface.[12]

Next, the average orientation of microcrystallites in the films was estimated from XRD intensities of the (h00) planes. The orientation factor, f, were calculated.[13] Results are seen in Table 2. Here, f is defined by

$f = (P - P_0) / (1 - P_0)$

where P is the fraction of diffraction intensity, I (h00) from the (h00) planes to the total intensities, ΣI (hkl), given as

$P = \Sigma I(h00) / \Sigma I(hkl)$

where P_0 is the value of P for the bulk. f varies from 0 (nonoriented) to 1 (completely oriented). If a thin film grows as polycrystalline, f may be used as an indicator of the grain orientation. With the reflection of the result of P, every f value of LBMO films is larger than that of the LBMO bulk. In all films the orientation to the substrate was confirmed, and each orientation is shown in Table 2. A film on a substrate having a small substrate-film mismatch seems to show a high orientation since the film is directly influenced on the substrate orientation. Especially, for the LBMO/STO film and the LBMO film deposited on LAO (the LBMO/LAO film), each X-ray double-crystal rocking curve at (200) was required in order to clarify the relative orientation of two films. The results are shown in Figs. 5(a), 5(b). Each curve is separated into a complex waveform drawn by solid lines. The differential angles between two peaks are $\Delta\theta$ 1 and $\Delta\theta$ 2. $\Delta\theta$ 1 in Fig. 5(a) is the angle for the LBMO/STO film, and $\Delta\theta$ 2 in Fig. 5(b) is the angle for the LBMO/LAO film. The relationship between the two angles is $\Delta\theta\,1 < \Delta\theta\,2$. It was confirmed that the LBMO/STO film having the small mismatch showed the small angle slippage from the substrate. Then, the full-width at half maximum of the LBMO/STO film in Fig. 5(a), 0.026°, is smaller than that of the LBMO/LAO film in Fig. 5(b), 0.096°. It is considered that crystal grains of the LBMO/STO film grew so largely that the orientation degree is higher than that of other films.

The morphology of the surface was observed by the AFM. AFM images of LBMO films deposited on STO, LAO and MgO substrates are shown in Figs. 6(a), 6(b) and 6(c), respectively. The grain number in Figs. 6(a)-6(c) is counted, and the relationship between the grain number (per square micron) and resistivity at room temperature is shown with the substrate-film lattice mismatch in Fig. 7. The large grain size

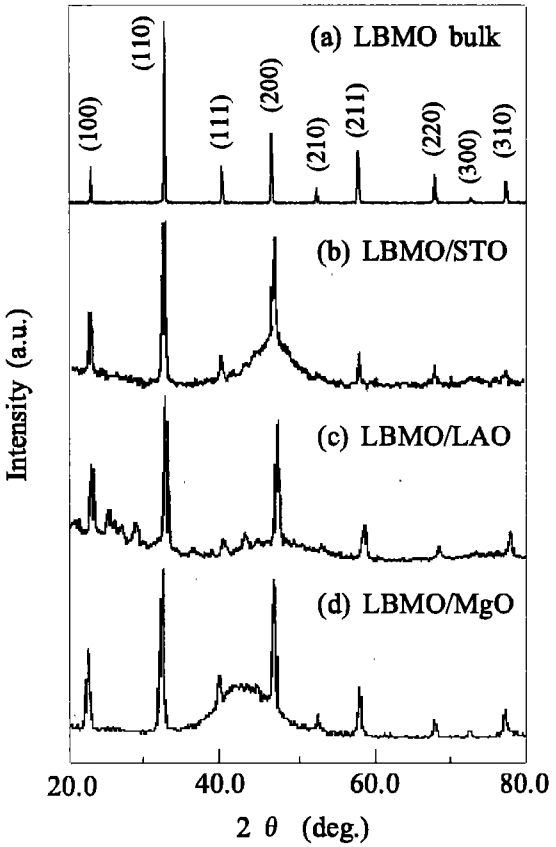

Fig. 4. XRD patterns of (a) the LBMO bulk, LBMO thin films deposited on (b) STO (100), (c) LAO (100) and (d) MgO (100) substrate.

Table 1. Lattice parameters of $La_{0.7}Ba_{0.3}MnO_{3-\delta}$ (LBMO) thin films on different substrate materials, $SrTiO_3$ (STO), $LaAlO_3$ (LAO) and MgO.

Lattice constant		Lattice mismatch	
Substrate (nm)	Film (nm)	Substrate-bulk (%)	Substrate-film (%)
STO 0.3905	0.3896	0.28	0.23
LAO 0.3790	0.3869	-2.67	-2.08
MgO 0.4211	0.3911	8.14	7.12
(LBMO bulk	0.3894)		

Table 2. The fraction of diffraction intensity P and the orientation factor f of each LBMO thin films on different substrates materials, $SrTiO_3$ (STO), $LaAlO_3$ (LAO) and MgO.

Substrate	P	f
STO	0.413	0.263
LAO	0.410	0.260
MgO	0.401	0.248
LBMO bulk	0.204 ($=P_0$)	0

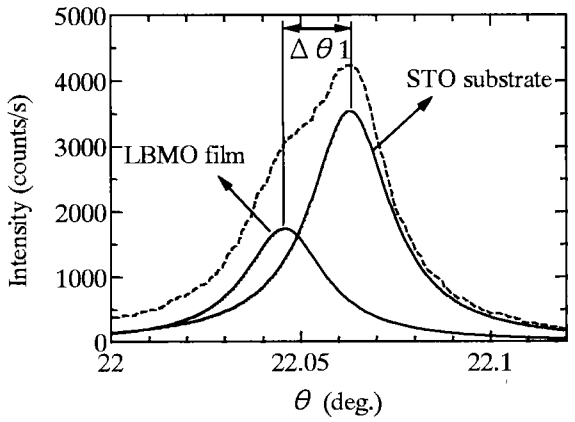

(a) LBMO/STO film

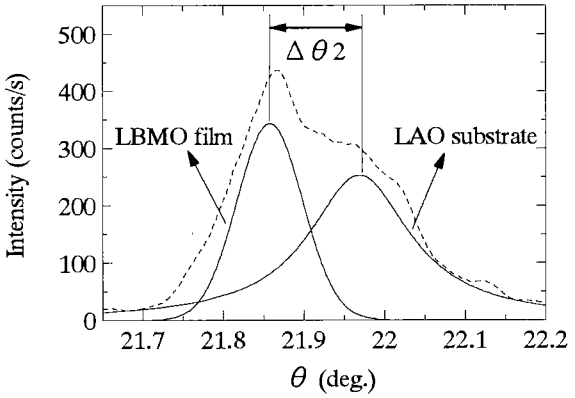

(b) LBMO/LAO film

Fig. 5. Rocking curves for the (200) peak of (a) the LBMO/STO film and (b) the LBMO/LAO film. The broken lines indicate the raw spectra. The double-headed arrows show the differential degree between the two peaks.

means that the number of grains and grain boundaries is little. Little grain boundaries seem that the resistivity of the LBMO/STO film is low in Fig. 7, because the conduction electrons are easily scattered at the grain boundaries.[14],[15] The grain of the LBMO/STO film is almost constant and large, whose diameter about 140 nm in Fig. 6(a). For the LBMO/LAO film in Fig. 6(b), some grains are larger than those of the LBMO/STO film, but various width grain boundaries are mixed. So, the average grain size can be considered to be smaller than that of the LBMO/STO film. Therefore, it seems that the resistivity of the LBMO/LAO film is much higher than that of the LBMO/STO film. The grain size of the LBMO/MgO film is about 50 nm in Fig. 6(c). Grains and grain boundaries of the LBMO/MgO film exist so many that the resistivity is high in Fig. 7. As a result, the grain number which affects the resistivity of LBMO films is changed by the substrate-film lattice mismatch.

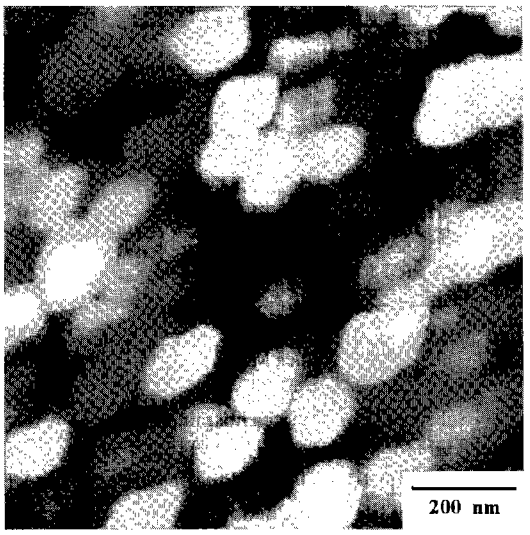

(a) LBMO/STO film

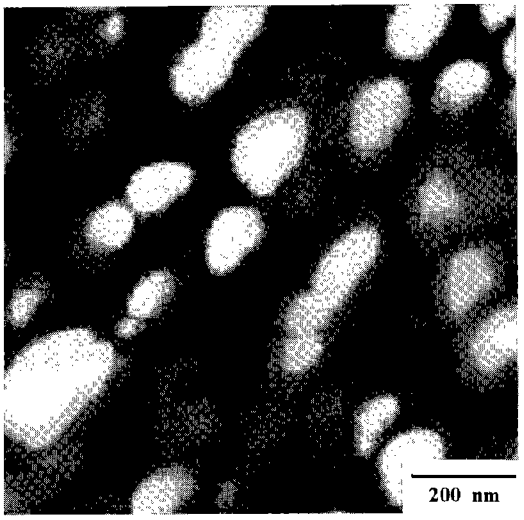

(b) LBMO/LAO film

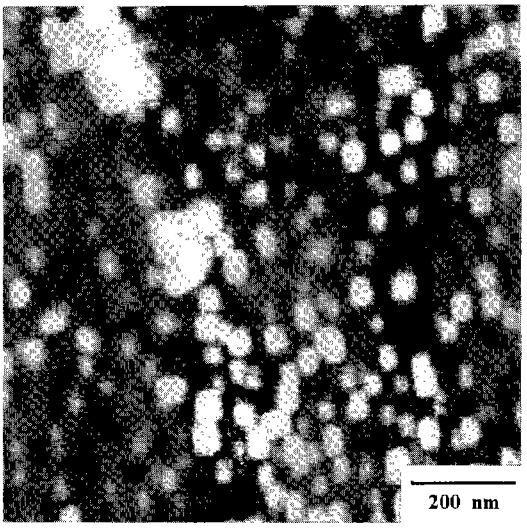

(c) LBMO/MgO film

Fig. 6. $(1\ \mu\mathrm{m})^2$ AFM images of LBMO films deposited on (a) STO (100), (b) LAO (100), (c) MgO (100) substrates.

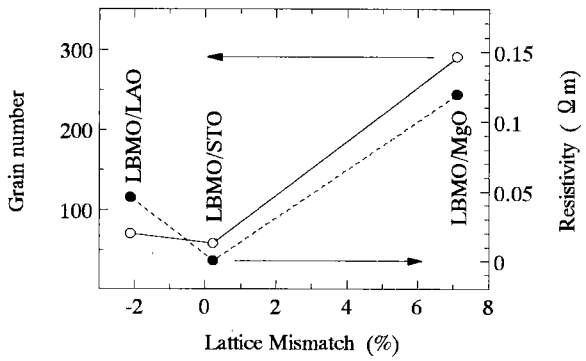

Fig. 7. Substrate-film lattice mismatch dependence of grain number [counted in Figs. 6(a)-6(c)] and resistivity at room temperature for the LBMO/STO film, the LBMO/LAO film and the LBMO/MgO film deposited under an oxygen pressure of 53.3 Pa.

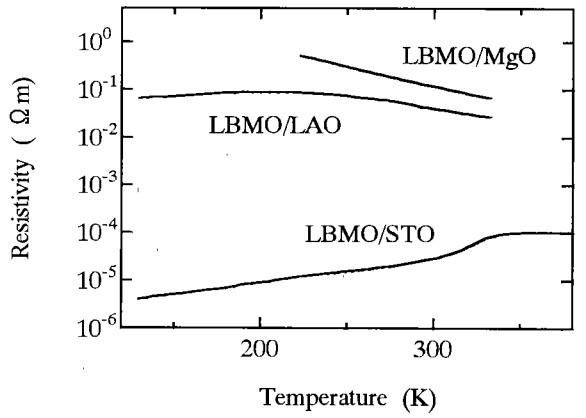

Fig. 8. Temperature dependence of resistivity for the LBMO/STO film, the LBMO/LAO film, and the LBMO/MgO film, which deposited under an oxygen pressure of 53.3 Pa.

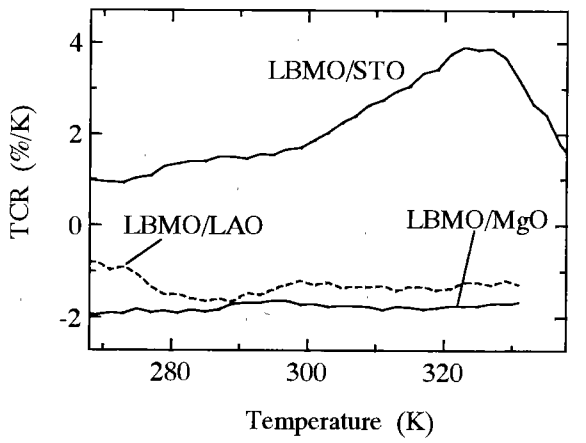

Fig. 9. Temperature dependence of TCR for the LBMO/STO film, the LBMO/LAO film and the LBMO/MgO film deposited under an oxygen pressure of 53.3 Pa.

3.3 **Resistivity and TCR** Fig. 8 shows temperature dependence of resistivity for the LBMO/STO film, the LBMO/LAO film and the LBMO/MgO film. The resistivity of the LBMO/STO film indicates its peak value about 365K. Below 365K the resistivity decreases with decreasing temperature. It is considered that there is the transition from paramagnetic insulator to ferromagnetic metal (the I-M transition) near resistivity peak temperature (Tp). This behavior of the LBMO/STO film with larger grain size agrees with that of previously reported in bulk samples.[16] In the case of the film with reduced grain size such as the LBMO/LAO film, Tp translates to lower temperature and its resistivity is three orders higher than that of magnitude of the LBMO/STO film.[17] Moreover, for the LBMO/MgO film having the smallest grains, Tp disappears and its resistivity is similar to an insulator.

Fig. 9 shows the temperature dependence of TCR for LBMO films deposited on STO, LAO and MgO, respectively. For the LBMO/STO film, the I-M transition seems to be above room temperature, and the gradient of resistivity d ρ/dT in Fig. 8 is positive like that of a metal. Thus large positive TCR values (the maximum is 4 %/K) are observed, and from 300K to 335K, TCR values of the LBMO/STO film is over 2 %/K. The TCR value of a conventional vanadium oxide bolometer is about 2 %/K,[10] so that the LBMO/STO film is considered to be a candidate for an uncooled bolometer material. But for the LBMO/LAO film and LBMO/MgO film, negative d ρ/dT is shown at near-room temperature. Absolute TCR values of these films are less than 2 %/K in Fig. 9.

4. Conclusion

The LBMO/STO film deposited under an oxygen pressure of 53.3Pa showed the (100)-orientation, since the substrate-film lattice mismatch was minute. And the film whose crystal grain size was about 140 nm showed the temperature dependence of resistivity like a LBMO bulk. Not only the film indicated high TCR values, about 4 %/K, at near-room temperature, but also its TCR values were over 2 %/K in wide temperature range of near room temperature. The LBMO/STO film is considered to be a candidate for an uncooled bolometer material from its TCR property. On the other hand, for LBMO films deposited on LAO and MgO substrates, the growth of the crystal grain was suppressed because of the large substrate-film lattice mismatch.

For the cost reduction of uncooled infrared bolometers, bolometers should be deposited on a conventional substrate, such as SiO_x, at low temperature without annealing. In the future, we will utilize this substrate-film mismatch effect and some doping materials to optimize the preparation condition.

(Manuscript received February 15, 2001, revised May 16, 2001)

References

(1) K. Chahara, T. Ohno, M. Kasai, and Y. Kozonoi, Appl. Phys. Lett. **63**, 1990 (1993).
(2) G. H. Jonker, and J. H. van Santen, Physica **16**, 337 (1950).
(3) C. Zener, Phys. Rev. **82**, 403 (1951).

(4) P. W. Anderson, and H. Hasegawa, Phys. Rev. **100,** 675 (1955).
(5) P. G. de Gennes, Phys. Rev. **118,** 141 (1960).
(6) H. L. Ju, J. Gopakakrishnan, J. L. Peng, Qi Li, G. C. Xiong, T. Venkatesan, and R. L. Greene, Phys. Rev. **B51,** 6143 (1995).
(7) P. G. Radaelli, M. Marezio, H. Y. Hwang, S. -W. Cheong, and B. Batlogg, Phys. Rev. **B54,** 8992 (1996).
(8) A. Goyal, M. Rajeswari, R. Shreekala, S. E. Lofland, S. M. Bhagat, T. Boettcher, C. Kwon, R. Ramesh, and T. Venkatesan, Appl. Phys. Lett. **71,** 2535 (1997).
(9) M. Nagashima and H. Wada, J. Mater. Res. **12,** 416 (1997).
(10) B. Meyer, R. Cannata, A. Stout, A. Gin, P. Taylor, E. Woodbury, J. Deffner and F. Ennerson: Proc. SPIE **2746,** 13 (1996).
(11) K. Hayashi, E. Ohta, and H. Wada, submitted to Proc. SPIE.
(12) E. Gommert, H. Cerva, J. Wecker, and K. Samwer, J. Appl. Phys. **85,** 5417 (1999).
(13) F. K. Lotgering, J. Inorg. Nucl. Chem. **9,** 113 (1959).
(14) W. Zhang, W. Boyd, M. Elliot, and W. H. Harkerand, Appl. Phys. Lett. **69,** 3929 (1996).
(15) K. -K. Choi, and Y. Yamazaki, Jpn. J. Appl. Phys. **38,** 56 (1999).
(16) R. von Helmolt, J. Wecker, K. Samwer, L. Haupt, and K. Barner, J. Appl. Phys. **76,** 6925 (1994).
(17) J. Rivas, L. E. Hueco, A. Fondado, F. Rivadulla, and M. A. Lopez-Quintela, J. Magn. & Magn. Mater. **221,** 57 (2000).

Ken-ichi Hayashi (Non-member) received the M.S. degree in physics from Nagoya University in 1995. He joined Japan Defense Agency in 1996. He is currently Ph.D. student in materials science of Keio University. He is a member of the Physical Society of Japan and the Japan Society of Applied Physics.

Eiji Ohta (Non-member) received the Dr. degree in instrumentation engineering from Keio University in 1979, and is presently a professor at the department of Applied Physics and Physico-Informatics of Keio University. He has worked on analysis and evaluation on semiconductor materials. He is a member of the Japan Society of Applied Physics, the Physical Society of Japan, and the Surface Science Society of Japan.

Hideo Wada (Member) received the BS. and MS degrees in electronics and in physics from the National Defense Academy, Kanagawa, Japan, in 1980 and 1985, respectively and received the Dr. degree in electronics from Science University of Tokyo in 1991. He joined Japan Self Defense Agency in 1980. In 1988, he joined R&D Center in Mitsui Mining & Smelting Co., LTD, Saitama, Japan, where he had been engaged in research on thermoelectric devices and semiconductor inspection systems. In 1993, he joined Technical Research and Development Institute, Japan Defense Agency, where he has been engaged in research on infrared device. He is currently a chief of Fourth electro-optical Laboratory of Third Division in the Second Research Center. He is a member of SPIE, the Electrical Engineers of Japan, the Japan Society of Applied Physics and Japan Society of Infrared Science and Technology.